Comparative analysis of wind turbine erosion using reanalysis, satellite and ground-measured rain data

Sanshodhan Shende[1], Alessio Castorrini[1,6], Charlotte Bay Hasager[2] , Abhiram Vinod[2] , Krystallia Dimitriadou[2], Elisa Adirosi[3], Giandomenico Pace [4], Lorenzo De Silvestri[4], Fernando Sánchez[5], Matthew S. Rose[6] and M. Sergio Campobasso[6]

[1]Sapienza University of Rome, Rome, Italy
[2]Department of Wind and Energy Systems, Technical University of Denmark, Roskilde, Denmark
[3]Institute of Atmospheric Sciences and Climate, National Research Council (CNR-ISAC), Italy
[4]Italian National Agency for New Technologies, Energy and Sustainable Economic Development (ENEA), Italy
[5]Research Institute of Design, Innovation and Technology, University CEU Cardenal Herrera, Valencia, Spain.
[6]School of Engineering, Lancaster University, Lancaster, United Kingdom

E-mail: `sanshodhan.shende@uniroma1.it`

Abstract. This work investigates leading edge erosion risk from the combined statistics of wind and rain at three sites (two offshore and one onshore). Coating lifetime for a reference 15 MW wind turbine is estimated using a rain erosion model driven by measured wind data and alternative rainfall inputs. Measurements include site-specific disdrometer and anemometer records, buoy-mounted offshore LiDAR, and satellite precipitation (IMERG-F). These datasets are systematically compared with ERA5 reanalysis to quantify meteorological discrepancies and their impact on erosion predictions. The overall objective is to evaluate the accuracy of large-scale global rainfall datasets for leading edge erosion prediction, since reliable erosion forecasts are essential for effective predictive maintenance and precipitation-reactive control strategies [1], and disdrometric measurements are rarely available at wind farm sites.

1. Introduction

Wind energy plays an essential role in decarbonization efforts, with offshore installations in continuous expansion thanks to consistently strong wind resources and sea space availability. To meet current capacity targets, turbines must not only increase in size and efficiency, but their degradation mechanisms also need careful management, since these directly affect performance and O&M costs [2]. Blade leading edge erosion (LEE), caused by repeated high-speed impacts of raindrops and other hydrometeors, is a critical issue [3] that progressively reduces aerodynamic efficiency and energy yield [4, 5] and can compromise structural integrity [6]. The assessment of LEE is therefore essential in both the planning and O&M of wind farms, relying on accurate characterization of wind and precipitation as well as reliable models for predicting the durability of leading edge protection systems [7].

A significant body of research has focused on evaluating LEE using measured wind and precipitation data, providing insights into turbine durability under real atmospheric conditions. Verma et al. [8, 9] combined measured rainfall and wind data with the Springer erosion model [10] to derive distributions of key rain parameters, highlighting the sensitivity of coating lifetime predictions to local atmospheric conditions. Letson et al. [11] employed measured drop size distributions in an energy-based model to quantify cumulative erosion damage, while Prieto et al. [12] integrated measured meteorological inputs with turbine operational data to characterize erosion severity across hydrometeor types. Castorrini et al. [7] proposed a framework predicting erosion lifetimes using measured environmental and material conditions, assessing

model formulation, data source, and material aging effects. Hasager et al. [13] applied measured datasets regionally across the North Sea and Baltic Sea, quantifying coating lifetime variations and economic impacts. Martinez et al. [14] used measured operational and inspection data to predict remaining blade life, conceptually aligned with LEE assessment. These studies demonstrate the central role of measured datasets in understanding and validating LEE.

These analyses depend on high-resolution local measurements, including those of rain and wind sensors, which are challenging to install and maintain offshore. This limitation motivates the use of alternative data sources, such as global reanalysis and satellite-based data, which provide wide spatial coverage and multi-year records. A number of studies have investigated LEE using reanalysis and model-based meteorological data to support offshore wind farm planning and maintenance where direct measurements are scarce. Contreras López et al. [15] developed frameworks combining ERA5 [16] and site observations with coating test data to estimate erosion evolution and energy losses, reporting annual energy production losses of 1.6 to 1.75% and first failures between 2 and 6 years. Hannesdóttir et al. [17] created a rain erosion atlas using ERA5, Norwegian Reanalysis Archive (NORA3) [18], and weather stations, finding LEE onset at about 5 years in Baltic Sea, and at about 3.2 years in the North Sea. Contreras López et al. [19] applied reinforcement learning with ERA5-informed weather data to optimize O&M, reducing costs by 12 to 21%. Visbech et al. [20] complemented these studies by investigating the dependence of LEE on wind speed and rain intensity using the New European Wind Atlas (NEWA) and GPM IMERG Final Precipitation L3 Half-Hourly product (IMERG-F V07B) [21] data, showing that neglecting the time-correlation of wind and rain data can overestimate the LEE incubation period by up to 90%. These studies demonstrate the role of reanalysis data for LEE assessment, while highlighting the importance of validation against measurements for offshore applications.

An important question, therefore, is whether reanalysis- and satellite-based rainfall estimates can be used reliably for LEE prediction when local rain measurements are not available. This study addresses this question by evaluating reanalysis- and satellite-based rainfall products through comparison of the resulting LEE predictions with those obtained using ground-based rainfall measurements, available at the considered sites. The analysis is conducted at three European sites representative of different climatic conditions: an onshore site in the UK and two offshore sites, one in the South Mediterranean and the other in the North Sea. To isolate the effect of using different rainfall sources, wind data are based exclusively on measurements. The study examines not only the resulting erosion predictions, but also the rainfall characteristics that drive the observed differences in coating degradation. This inter-site evaluation provides a critical benchmark for testing the robustness and operational reliability of reanalysis-driven erosion predictions. The structure of the paper is as follows: Section 2 describes the rain and wind data used; Section 3 recalls the methodology for rain erosion prediction; Section 4 presents the results, including site-specific erosivity analyses at the blade leading edge 4.1 and a sensitivity analysis of sampling interval on coating lifetime predictions 4.2.

2. Rain and wind data

The analysis of rain and wind data is carried out at three sites to compare the inputs used for the LEE assessment, including ground-based measurements (where available), ERA5 reanalysis, and IMERG satellite-based estimates. The aim is to evaluate the consistency of these datasets across different climatic conditions and to support the subsequent comparison of their impact on erosion predictions.

The first site ("Lancaster") is the onshore Hazelrigg location in Northwest England, situated within the Lancaster University premises, where a 2.3 MW wind turbine and a UK Met Office weather station are operational. The second site ("Lampedusa") is on the island of Lampedusa in the South Mediterranean, where the ENEA Station for Climate Observation is located. Lampedusa is a small island with an area of about 20 km^2, lying approximately 130 km from

Tunisia and 215 km from Sicily. The island has a fairly flat terrain, and the prevailing wind direction is from the northwest. The weather station, positioned on the northeastern coast, includes a 10-meter mast and a disdrometer. The third site ("North Sea") is offshore in the North Sea, off the western coast of Germany, where two buoys are equipped with a wind LiDAR and a weather station. In this case, the GPM IMERG Final Precipitation L3 Half-Hourly product (IMERG-F V07B) is used for rain data. The system provides near-global coverage at a $0.1^\circ \times 0.1^\circ$ spatial resolution and 30-minute temporal resolution. IMERG-F is recommended for research as it incorporates monthly gauge adjustments from the Global Precipitation Climatology Center (GPCC), enhancing the accuracy and reliability of precipitation estimates. Together, the three sites cover both onshore and offshore conditions across different European climates, giving a useful range of wind and rainfall regimes for assessing LEE. The coordinates, reference periods, and yearly rainfall for the three sites are reported in Table 1:

Table 1: Reference periods for LEE analyses at selected sites.

Site	Latitude	Longitude	Start date	End date	Rainfall [mm]
Lancaster	54.0138° N	2.7749° W	October 2018	September 2019	1193
Lampedusa	35.518° N	12.630° E	January 2024	December 2024	190
NS site	54.4029° N	5.5211° E	March 2022	February 2023	1260

The occurrences of rainfall rate, R [mm/hr], with 60-min sampling are compared across the three sites as rainfall rate is one of the most important parameters from the point of view of LEE. Three data sources are used for this analysis: measured rainfall from disdrometers at Lancaster and Lampedusa, ERA5 reanalysis data available for all three sites, and satellite-based precipitation from the GPM IMERG Final Precipitation L3 Half-Hourly product (IMERG-F V07B), which is also available for all the sites.

For the measured data at Lancaster and Lampedusa, rainfall is obtained from Thies Clima^{TM} LPM disdrometers, which measure droplet diameters in 22 classes from 0.125 mm and terminal velocities in 20 classes from 0 m/s [22]. The measured droplet size distribution (DSD) $N_M(D)$ for each 1-min interval is computed as

$$N_M(D_i) = \frac{1}{Av_t(D)\Delta t}\frac{\Delta n_i}{\Delta D_i}, \tag{1}$$

where D_i, ΔD_i and Δn_i are the mean diameter, width and number of drops of the i^{th} droplet class, $v_t(D)$ is the terminal velocity of droplets in that class, A is the instrument capture area, and $\Delta t = 60$ s. All diameters are in mm, v_t in m/s, A in m^2, and N_M in [mm^{-1} m^{-3}]. Measured 1-min droplet size and velocity data are filtered based on the empirical terminal velocity relationship [23, 24, 25]:

$$v_t(D) = 9.65 - 10.3e^{-0.6D}, \tag{2}$$

removing droplets with measured velocities deviating by more than 50% from this value. The rainfall rate R [mm/hr] for each 1-min interval is then calculated as

$$R = \frac{3.6 \cdot 10^{-3}}{A\Delta t}\sum_{i=1}^{22}\Delta n_i V_i, \tag{3}$$

where V_i is the volume of a droplet with diameter D_i.

As reanalysis rainfall data, the total precipitation (tp) variable from the ERA5 dataset is used at all sites, with a 60-min sampling interval. Therefore, for the following comparisons, satellite-based IMERG-F data (provided over 30-min intervals) and disdrometric data (provided over 1-min intervals) are aggregated over 60-min intervals by averaging consecutive measurements.

For Lancaster, Figure 1a, the rainfall rate distributions derived from the disdrometer and the IMERG-F product exhibit strong agreement across the entire range of rainfall intensities, highlighting the consistency of the satellite-based precipitation estimates with high-resolution ground measurements. The ERA5 reanalysis data show satisfactory alignment with the disdrometer and IMERG distributions for rainfall rates up to approximately 2.5 mm/hr, although they consistently indicate slightly higher counts in this range. Beyond 2.5 mm/hr, ERA5 underestimates the frequency of higher rainfall rates, leading to reduced correspondence with the other two datasets. At the Lampedusa site (Figure 1b), the IMERG-F and ERA5 rainfall rate distributions show comparatively good agreement. In contrast, the disdrometer-based measurements report lower rainfall frequencies up to about 1.5 mm/hr. Beyond this threshold, only a few occurrences of high-intensity rainfall in the hourly sampling are recorded in the measured data, resulting in limited overlap with the satellite- and reanalysis-based distributions. The observed differences between disdrometric measurements and satellite and reanalysis products may be due to the prevalence of convective rainfall at Lampedusa. This precipitation type is characterized by relatively large droplet diameters and localized events, which can reduce the ability of coarse-resolution data sources to accurately capture rainfall occurring at the disdrometer location.

Comparison of IMERG-F data with ERA5 at the North Sea site illustrated in Figure 1c shows good agreement up to $R \approx 3$ mm/hr, while ERA5 underestimates occurrences at higher rainfall rates.

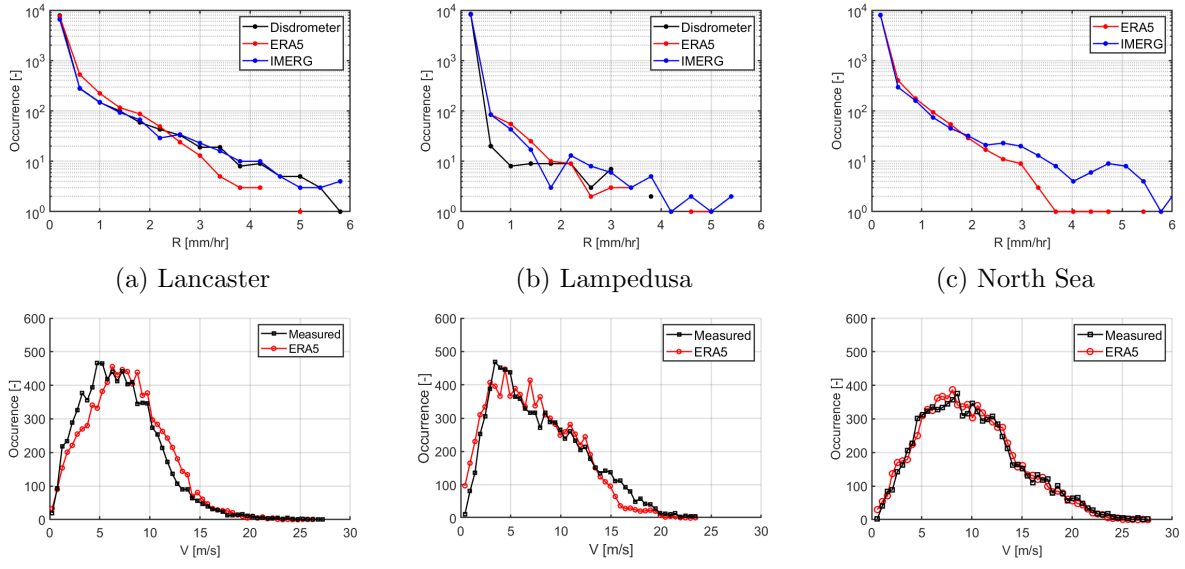

(a) Lancaster (b) Lampedusa (c) North Sea

(d) Lancaster (e) Lampedusa (f) North Sea

Figure 1: Comparison of measured and reanalysis-based distributions of rainfall rates (a, b, c), and occurrence of wind speed (d, e, f) at the three sites.

The occurrence diagrams of the wind speed over the reference period are shown in the bottom plots of Figure 1. The plots compare measured wind speed data aggregated over 1 hr intervals and the ERA5 wind speeds at a height of 150 m.

At Lancaster and North Sea sites, the original measurement frequency is 10 minutes; therefore, six consecutive 10-minute values are averaged to obtain 60-minute data. At Lampedusa, the measurements are available at a 1-min frequency, and each set of sixty consecutive 1-min values is averaged to achieve a common hourly resolution.

A standard power law is applied across all sites to derive wind speeds at 150 m. In all cases,

the wind shear exponent γ is dynamically computed for each sampling interval. For Lancaster and Lampedusa, γ is derived from ERA5 wind speeds at 10 m and 100 m, whereas for the North Sea site it is obtained directly from the measured LiDAR wind speeds at 140 m and 200 m. The annual average wind speeds at 150 m height for all datasets are reported in Table 2. At all three sites, both the measured and ERA5 wind speed datasets show good agreement. This level of agreement suggests that both datasets are adequate for the LEE analysis and capture the wind conditions of the reference periods reasonably well. In all erosion calculations presented in this study, the measurement-based wind speeds are used. This is done to focus solely on assessing the sensitivity of the LEE analyses to the uncertainty affecting rain data. The precipitation data are always synchronized with the measured wind by matching their timestamp. This enables using synchronous time-series of wind and rain data.

Table 2: Mean wind speeds at 150 m height from measured and ERA5 data at the three sites.

Site	Mean Measured Wind Speed (m/s)	Mean ERA5 Wind Speed (m/s)
Lancaster	7.11	7.71
Lampedusa	8.00	7.31
North Sea	9.93	9.76

3. Methodology for rain erosion

The durability of the blade leading edge material is assessed using the methodology and modeling framework described in the DNV-RP-0573 recommended practice, which improves the approach of Springer [10] by incorporating experimental data from Whirling Arm Rain Erosion Tests (WARET). The methodology calibrates the critical parameters of the original model using fatigue-type relations based on WARET data, relating the droplet impact speed to the number of impacts N required to reach the end of the incubation period.

Here, only the main data and features used in the case study are reported; a detailed description of the models and methods can be found in DNV-RP-0573 and [7], where the approach is implemented and evaluated using different setups and model variants for material characteristics and droplet impingement. The results in [7] showed that, for the case study therein, using a WARET-based approach instead of a fundamental material property-based one yields incubation times about 50% longer, and that neglecting aerodynamic droplet slowdown or including UV-induced weathering changes the predicted erosion life by about 12% and 30%, respectively. In the present study, we focus on the sensitivity of the LEE analysis to the variability of rain data arising from using different data sources.

The material data used in this study refer to the 3M W4600 liquid coating analyzed in [26]. The material properties are summarized in Table 3, the WARET operating conditions are reported in Table 4, and the measured fatigue parameters are provided in Table 5.

Table 3: Leading edge protection configuration and material stress wave parameters for the reference material 3M W4600 coating system.

Material Stress Wave Parameters	Coating	Substrate	Water
Density (kg/m^3)	ρ_c 1100	ρ_s 1560	ρ_L 1000
Speed of Sound (m/s)	C_c 1900	C_s 2098	C_L 1480
Acoustic Impedance (kg/m^2/s)	Z_c 2090000	Z_s 3272880	Z_L 1480000
Coating Thickness (mm)	h_c 0.175	—	—

Table 4: Testing operational parameters for the 3M W4600 coating system.

Parameter	Value
Mean droplet diameter ϕ (mm)	2.25
Impact speed v (m/s)	134
Impact angle θ (°)	90
Rain intensity I (mm/h)	31.34

Table 5: Material fatigue parameters for the 3M W4600 coating system.

Parameter	Coating
Poisson ratio ν	0.3
Ultimate tensile strength σ_u (MPa)	3.7×10^7
Fatigue slope parameter b	16.92

4. Results

4.1. Analysis of site erosivity at the blade leading edge

The LEE risk at the Lancaster, Lampedusa and North Sea sites is assessed using the IEA 15 MW reference wind turbine [27]. The incubation time (material durability), corresponding to the onset of erosion, is evaluated at six radial blade positions (r), reported both as percentages of the tip radius (R) and distance in meters from the rotor axis in Table 6, also providing the chord length (c) at the six positions.

Table 6: Positions at which LEE analyses are performed and corresponding blade chords.

r [%]	70	75	80	85	90	95
r [m]	84.68	90.73	96.78	102.82	108.87	114.92
c [m]	3.22	3.00	2.77	2.52	2.26	1.99

As LEE depends on the combined characteristics of wind speed and rain DSDs, these are compared using joint frequency distribution functions (FDFs) of droplet relative frequency, with the resulting impact on erosion illustrated by the corresponding fractional damage[7]. Figure 2 presents these comparisons. The relative frequency $n_v/n_{v,T}$ is the ratio of the number of droplets per m^3 n_v in a given V–D bin, (where V is the wind speed and D the droplet diameter in mm) to the total number of droplets per m^3 $n_{v,T}$ over the reference period. The fractional damage $D_s/D_{s,T}$ is the ratio of the erosion damage D_s caused by all droplets in a given V–D bin to the total cumulative damage $D_{s,T}$, here evaluated at blade position with $r = 0.95R$.

Disdrometers provide measured DSDs at Lancaster and Lampedusa, whereas at the North Sea site the DSD is derived from IMERG and ERA5 rainfall rates using Best's model [28]. For Lancaster and Lampedusa, three rainfall datasets are employed: disdrometer-based, IMERG and ERA5. For the North Sea site, only IMERG and ERA5 rainfall data are available. All available data are used to perform the LEE analysis and assess the variability in coating lifetime predictions arising from different rainfall sources. The results of this comparative analysis are visualized in Figure 3.

The results indicate a consistent trend across all sites, with coating lifetime (here the incubation time) decreasing along the length of the blade for each dataset. Based on measured DSDs, LEE at Lancaster is substantially higher than at Lampedusa, as lifetime at 95% tip radius is approximately one year in the former case, and 13.9 years in the latter. This difference is due to two factors: firstly, the annual rainfall at Lancaster in the reference period is about six times larger than at Lampedusa (Table 1), and secondly, a considerable portion of rainfall at Lampedusa occurs under low wind speed conditions, which are less critical because of the lower rotor tip velocity. The North Sea site exhibits the largest erosivity, with an average coating lifetime of about 0.75 years. This is because this site shows the highest annual rainfall and the largest fraction of intense precipitation at high wind speeds.

For Lancaster, the coating lifetime predictions based on measured DSDs and IMERG rainfall data are closely aligned, with values of 1.0 and 1.1 years, respectively, at the outermost blade

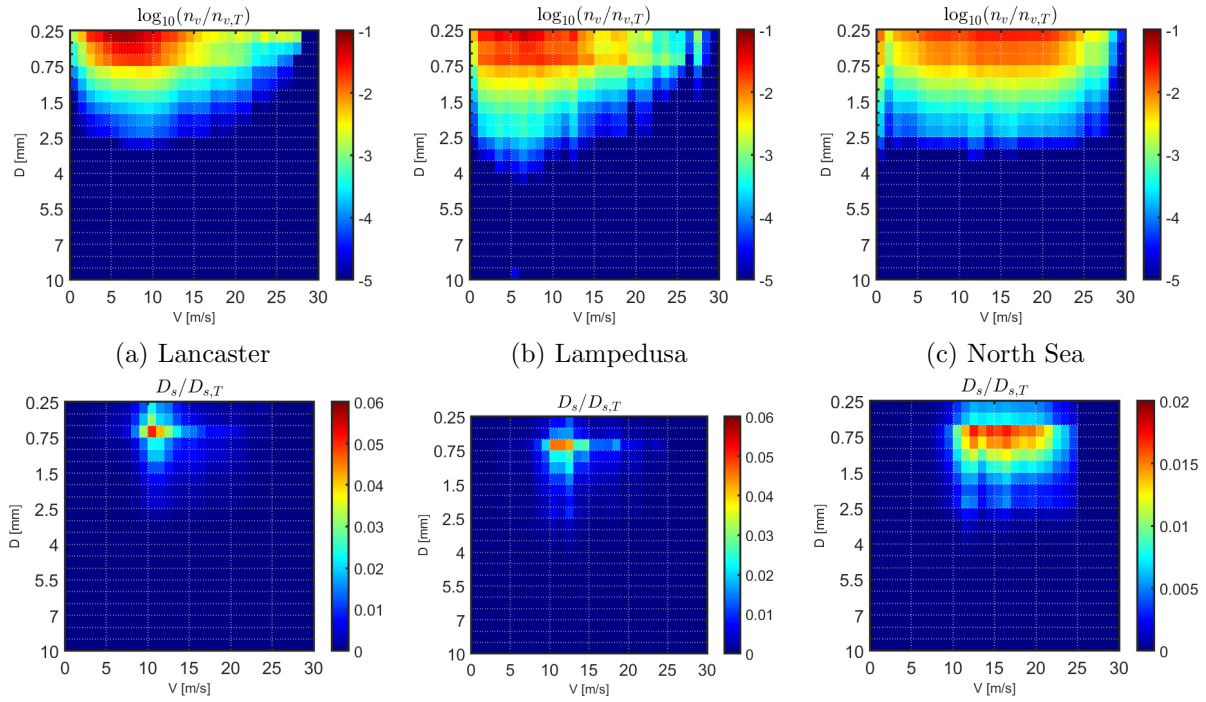

(a) Lancaster (b) Lampedusa (c) North Sea

(d) Lancaster (e) Lampedusa (f) North Sea

Figure 2: Droplet relative frequency distributions (a, b, c) and corresponding fractional damage distributions at $0.95R$ (d, e, f) for the three sites.

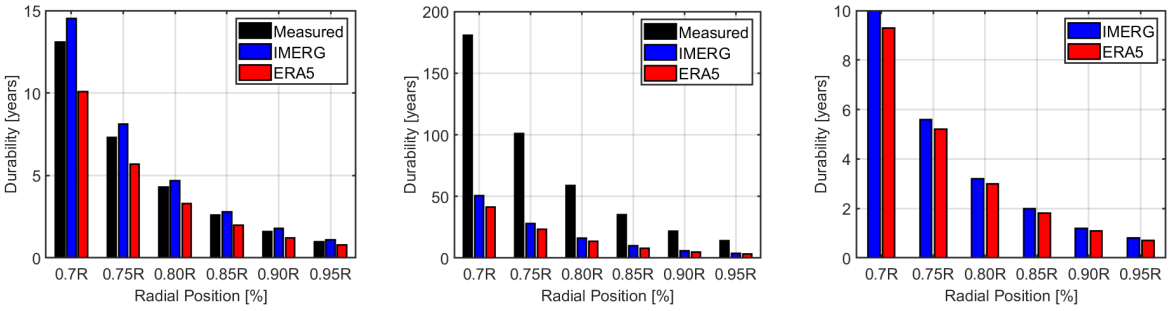

(a) Lancaster (b) Lampedusa (c) North Sea

Figure 3: Predicted coating lifetime at six radial positions along the turbine blade for all three study sites.

position. In comparison, the ERA5 dataset yields a slightly lower lifetime of 0.8 years, reflecting a modest underestimation relative to the other two datasets. For Lampedusa, the measured dataset predicts a substantially longer coating lifetime, reaching 13.9 years at the outermost blade position, compared to 3.9 years for the IMERG dataset and 3.2 years for ERA5. This significant difference arises from the discrepancies in rain data observed in Figure 1b at lower rainfall rates, between 0.5 and 1.5 mm/hr. Indeed, at these rates the average droplet size computed with Best's formulation [28] falls within the range of maximum specific damage shown in Figure 2e, indicating that this regime contributes a significant share to the overall damage prediction. Any bias or deviation in the reanalysis rainfall rate is therefore carried into the derived DSD and subsequently into the lifetime calculation. This effect becomes more

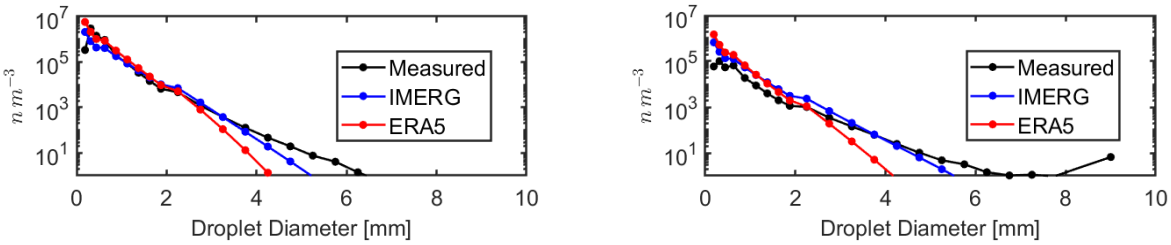

(a) Lancaster (b) Lampedusa

Figure 4: Comparison of number of droplets per m^3 obtained from disdrometer vs. those derived from IMERG and ERA5 rainfall data.

important for Lampedusa, where the overall rainfall is much lower than at Lancaster, making the DSD generation more sensitive to variations in the underlying rainfall rate. To further examine whether these differences arise from rainfall-rate discrepancies or from the DSD reconstruction from Best's model, the total number of droplets per m^3 derived from IMERG and ERA5 rainfall is compared with that obtained from the disdrometer. Figure 4 shows that the agreement between measured data and those derived from IMERG and ERA5-based distributions is generally good, particularly at Lancaster, whereas somewhat larger deviations appear for Lampedusa. The values of total annual rainfall are as follows: at Lancaster the measured total rainfall is 1193 mm, compared with 1454.67 mm from ERA5 and 1195.66 mm from IMERG, whereas at Lampedusa the measured total rainfall is 190 mm, compared with 305.67 mm from ERA5 and 386.78 mm from IMERG.

For the North Sea site, the coating lifetime predicted by the IMERG dataset is slightly higher than that from ERA5, with values of 0.8 and 0.7 years respectively. The small difference between the two datasets indicates a close agreement in predicted durability, suggesting consistent rainfall characterization between the two sources for this site.

The agreement with the LEE predictions obtained using disdrometric rainfall measurements at the Lancaster and Lampedusa sites can be used to compare the reliability of using IMERG and ERA5 datasets in LEE analysis. In particular, better agreement at both sites is obtained when the LEE analysis is based on IMERG rainfall data rather than ERA5 rainfall data. Relative to the disdrometer-based estimate, the differences in predicted coating lifetime are 10.7% for IMERG-based predictions and 22.8% for ERA5-based predictions at Lancaster, and 72.1% and 77.1%, respectively, at Lampedusa.

4.2. Sensitivity analysis of time resolution on coating lifetime prediction

Since meteorological datasets are often available at varying temporal resolutions, the following sensitivity analysis examines how the time resolution of the input data affects the LEE predictions. To simulate this effect with the available data, rainfall measurements from disdrometers at Lancaster and Lampedusa, together with measured wind data extrapolated to hub height, were aggregated over a range of temporal intervals to assess the robustness of the coating lifetime predictions when only coarse temporal resolutions (such as 30-min for IMERG and 60-min for ERA5) are available.

Figure 5 presents a comparison of rainfall rate distributions for Lancaster and Lampedusa at 60-min and 30-min aggregation intervals, based on IMERG and disdrometric data. The occurrence-based plots show that the same qualitative differences between the datasets persist when switching from 60-min to 30-min sampling. Indeed, where the agreement of the IMERG data is strong (Lancaster site), it maintains the same trend when increasing the temporal resolution. In contrast, for Lampedusa, smaller differences are observed in the range of low and medium rainfall rates, but distributed over a wider range, indicating that increasing the

time resolution (i.e., reducing temporal aggregation) improves accuracy, as rainfall at this site is characterized by more localized events in time.

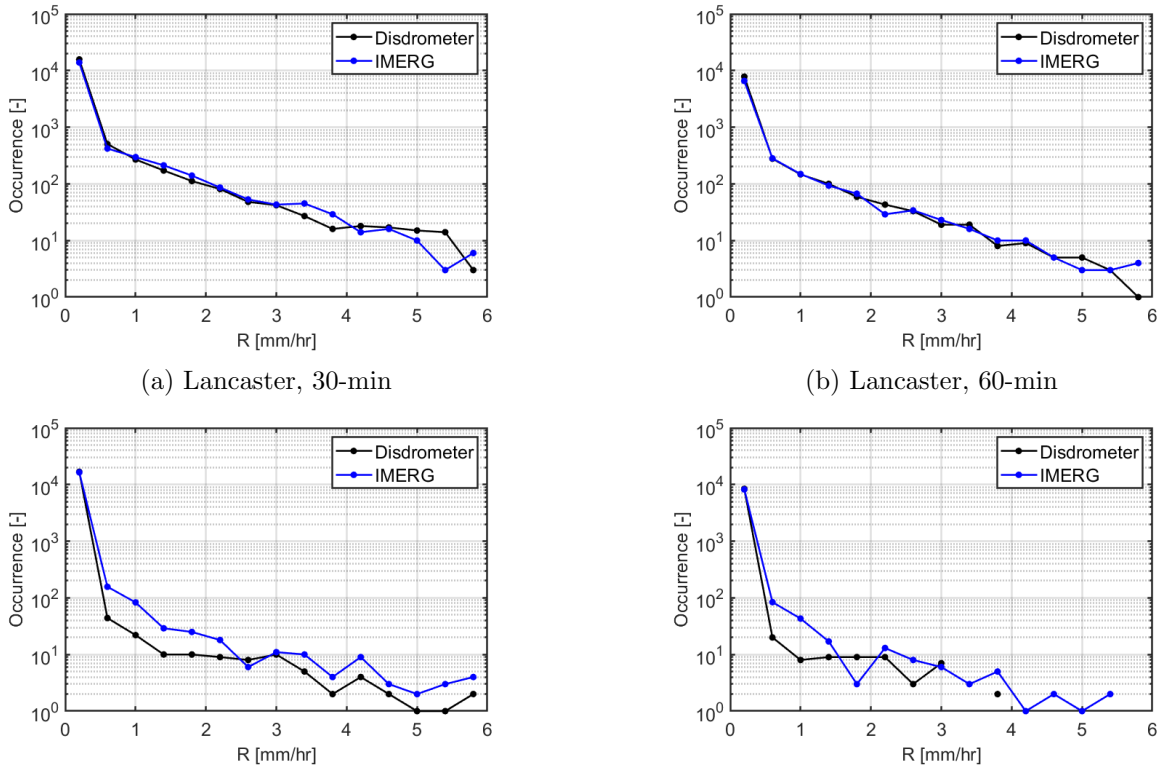

(a) Lancaster, 30-min

(b) Lancaster, 60-min

(c) Lampedusa, 30-min

(d) Lampedusa, 60-min

Figure 5: Rainfall rate distributions at two temporal resolutions (30-min and 60-min) for Lancaster and Lampedusa.

Table 7 reports the coating lifetime predictions as a function of the time-resolution of the rainfall rate at Lancaster and Lampedusa, for $r = 80\%R$ and $r = 95\%R$, and for 1-min, 5-min, 10-min, 30-min, and 60-min resolution intervals. To interpret the results for the Lancaster site, it is first important to note that, for this site, measured wind data at 1-minute and 5-minute resolutions were not available. Consequently, the 10-minute wind speed data were replicated to populate the corresponding 1-minute and 5-minute time series. Since the same underlying 10-minute wind speed values were used in both cases, the average wind speeds remain identical. In addition, the rainfall contributing to the droplet size distribution is modified only through the applied temporal aggregation of the DSDs. As a result, for erosion-relevant calculations, the 1-minute and 5-minute inputs provide effectively equivalent information. This leads to predicted coating lifetimes that remain almost unchanged across these aggregation intervals. That said, the predicted coating lifetimes show relatively small variability across all the time resolutions under analysis.

For the Lampedusa site, the predicted coating lifetimes increase as the time-interval is increased, with a maximum difference of 8% between the 1-min and 60-min cases. As also shown in Figure 6, rainfall at Lampedusa is sporadic, with short and intense events. This feature is better captured by the disdrometer, whereas IMERG represents rainfall there as more continuous and temporally smoothed. This may explain the larger deviation of the IMERG-based LEE predictions from the disdrometer-based ones at this site, as well as the greater

sensitivity to temporal aggregation, which leads to a loss of information on the time correlation between intense rainfall and wind.

Table 7: Sensitivity of coating lifetime predictions to rainfall time resolution at Lancaster and Lampedusa for $r/R = 80\%$ and $r/R = 95\%$.

	Life [yr] - Lancaster					**Life [yr] - Lampedusa**				
r [%]	1 min	5 min	10 min	30 min	60 min	1 min	5 min	10 min	30 min	60 min
80	4.276	4.276	4.272	4.308	4.278	56.008	57.929	58.797	60.179	60.571
95	1.008	1.008	1.007	1.015	1.008	13.202	13.654	13.859	14.185	14.277

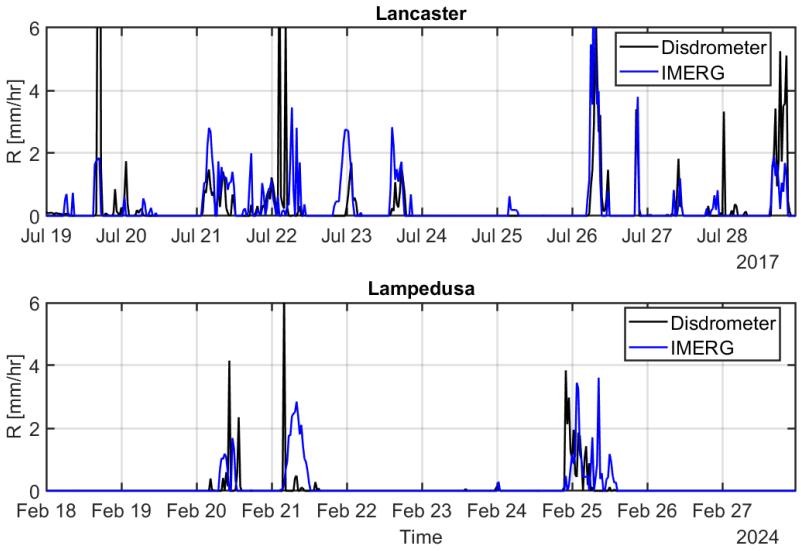

Figure 6: Time series comparison of 30 min sampled rainfall rates from the disdrometer and IMERG for Lancaster and Lampedusa.

To provide additional context for this behavior and to illustrate the underlying rainfall patterns at both sites, two time windows of rainfall rate were examined by comparing aggregated data on 30-min intervals from the disdrometer and IMERG, as shown in Figure 6. These series show that rainfall at Lampedusa occurs in shorter and more irregular bursts, making erosion predictions more sensitive to changes in the measurement interval. In contrast, Lancaster exhibits more continuous rain events, resulting in lower sensitivity of the results to temporal aggregation. The time series also indicate that rainfall events detected by the disdrometer generally coincide with those identified by IMERG at both locations, supporting the overall consistency between the two datasets in capturing rain occurrence. However, differences in rain intensity remain, with larger discrepancies at higher intensities, consistent with the reduced ability of satellite measurements to resolve localized convective rainfall events.

5. Conclusions

We compared LEE occurrence at one Northwest England onshore site (Lancaster) and two offshore sites, one in the North Sea and the other in the South Mediterranean (Lampedusa). Reanalysis- and satellite-derived rainfall data were used at all three sites, and disdrometric data were also used at the Lancaster and Lampedusa sites. The LEE assessments showed that Lancaster and North Sea sites exhibited broadly comparable coating lifetimes across datasets,

while Lampedusa displayed the largest LEE lifetime differences arising from using different rain data sources, due to its sparse and highly intermittent rainfall: substantially longer lifetimes were estimated using disdrometric measurements rather than ERA5 or IMERG. The analysis of the sensitivity of the predicted LEE lifetime to the time-resolution of the wind and rain data showed that Lancaster is largely insensitive to such temporal resolution, whereas Lampedusa shows a more noticeable dependence on this parameter, although the lifetime variations with the time-resolution are gradual and relatively small, confirming the robustness of the methodology. The obtained results indicate that reanalysis and satellite rain datasets can be used for LEE assessments when measurements are not available, with IMERG-based LEE analyses being closest to the measured DSD-based lifetimes at the sites where disdrometric data were available.

References

[1] Campobasso M S, Rose M S, Shende S, Adirosi E, Pace G, De Silvestri L, Dimitriadou K, Vinod A, Hasager C B, Sánchez F and Castorrini A 2026 *Renewable Energy* **262** 125357
[2] Rinaldi G, Thies P R and Johanning L 2021 *Energies* **14** ISSN 1996-1073
[3] Herring R, Dyer K, Martin F and Ward C 2019 *Renewable and Sustainable Energy Reviews* **115** 109382
[4] Cappugi L, Castorrini A, Bonfiglioli A, Minisci E and Campobasso M 2021 *Energy Conversion and Management* **245** 114567
[5] Campobasso M S, Castorrini A, Ortolani A and Minisci E 2023 *Renewable and Sustainable Energy Reviews* **178** 113254
[6] Castorrini A, Ortolani A and Campobasso M S 2023 *Renewable Energy* **218** 119256 ISSN 0960-1481
[7] Castorrini A, Barnabei V F, Domenech L, Šakalyté A, Sánchez F and Campobasso M S 2024 *Renewable Energy* **227** 120549
[8] Shankar Verma A, Jiang Z, Ren Z, Caboni M, Verhoef H, van der Mijle-Meijer H, Castro S G and Teuwen J J 2021 *Wind Energy* **24** 1315–1336
[9] Verma A S, Jiang Z, Caboni M, Verhoef H, van der Mijle Meijer H, Castro S G and Teuwen J J 2021 *Renewable Energy* **178** 1435–1455 ISSN 0960-1481
[10] Springer G S, Yang C I and Larsen P S 1974 *Journal of Composite Materials* **8** 229–252
[11] Letson F and Pryor S C 2023 *Energies* **16** 3906
[12] Prieto R and Karlsson T 2021 *Wind Energy* **24** 1031–1044
[13] Hasager C B, Vejen F, Skrzypiński W R and Tilg A M 2021 *Energies* **14** 1959
[14] Martinez C, Asare Yeboah F, Herford S, Brzezinski M and Puttagunta V 2019 *SMU Data Science Review* **2** 17
[15] López J C, Kolios A, Wang L and Chiachio M 2023 *Renewable Energy* **203** 131–141 ISSN 0960-1481
[16] Hersbach H, Bell B, Berrisford P and et al 2020 *Quarterly Journal of the Royal Meteorological Society* **146** 1999–2049
[17] Ásta Hannesdóttir, Kral S T, Reuder J and Hasager C B 2024 *Results in Engineering* **22** 102010 ISSN 2590-1230
[18] Haakenstad H, Breivik Ø, Furevik B R, Reistad M, Bohlinger P and Aarnes O J 2021 *Journal of Applied Meteorology and Climatology* **60** 1443–1464
[19] Lopez J C and Kolios A 2024 *Renewable Energy* **227** 120525 ISSN 0960-1481
[20] Visbech J, Hasager C B, Göçmen T and Réthoré P E 2025 *Renewable Energy* **253** 123358 ISSN 0960-1481
[21] Huffman G J, Stocker E F, Bolvin D T, Nelkin E J and Tan J 2023 Gpm imerg final precipitation l3 half hourly 0.1 degree x 0.1 degree v07 accessed: 2025-09-08
[22] THIES-Clima Laser Precipitation Monitor `https://www.thiesclima.com/db/dnl/5.4110.xx.x00_Laser_Precipitation_Monitor_eng.pdf` Adolf Thies GmbH, Göttingen, Germany. Accessed on 30 July 2025
[23] Atlas D, Srivastava R C and Sekhon R S 1973 *Reviews of Geophysics* **11** 1–35
[24] Adirosi E, Porcù F, Montopoli M, Baldini L, Bracci A, Capozzi V, Annella C, Budillon G, Bucchignani E, Zollo A L, Cazzuli O, Camisani G, Bechini R, Cremonini R, Antonini A, Ortolani A, Melani S, Valisa P and Scapin S 2023 *Earth System Science Data* **15** 2417–2429
[25] Tokay A, Wolff D B and Petersen W A 2014 *Journal of Atmospheric and Oceanic Technology* **31** 1276 – 1288
[26] Sánchez F, Hao H, Domenech L, Hardalupas Y, García V, Charalambides M, Ibáñez-Arnal M, Sergis A and Taylor A 2025 *Available at SSRN 5165106*
[27] Gaertner E e a 2020 Definition of the iea wind 15-mw offshore reference wind turbine Tech. Rep. NREL/TP-5000-75698 NREL Golden, CO, USA
[28] Best A C 1950 *Quarterly Journal of the Royal Meteorological Society* **76** 16–36